

## **Study on Resist Performance of Chemically Amplified Molecular Resists Based on Cyclic Oligomers**

Hiroki Yamamoto<sup>a\*</sup>, Kudo Hiroto<sup>b\*</sup>, Takahiro Kozawa<sup>a</sup>

<sup>a</sup> The Institute of Scientific and Industrial Research, Osaka University, 8-1 Mihogaoka, Ibaraki, Osaka 567-0047, Japan

<sup>b</sup>Materials and Bioengineering, Kansai University, 3-3-35 Yamate-cho, Suita, Osaka 564-8680, Japan

\*E-mail e-mail: [hiroki@sanken.osaka-u.ac.jp](mailto:hiroki@sanken.osaka-u.ac.jp)

Keywords: Chemically amplified resist, extreme ultraviolet, molecular resist, noria derivative, calixarene derivative

Novel resist materials are required for lithographic processing with ionization radiation such as extreme ultraviolet (EUV) and electron beam (EB) exposure tools. In this study, we synthesized positive-tone chemically amplified molecular resist materials with pendant adamantyl ester (AD) and cyclohexyl 2-propyl ether moieties based on cyclic oligomers such as noria, calixarene dimer, cyclodextrin, and pillar[5]arene, and we examined the lithographic performances of sensitivity, etching durability, and patterning under EUV and EB exposure. We clarified that the sensitivity of the resist materials was consistent with the structure of the cyclic oligomers, i.e., the hole size of the molecular structure might be an important factor relevant to high-resolution resist materials. We found that chemically amplified molecular resists based on cyclic oligomers such as noria, calixarene dimer, cyclodextrin, and pillar[5]arene are promising candidates for higher-resolution resist materials.

Corresponding Author

Tel: +81 6 6879 8502 / Fax: +81 6 6879 4889

\*E-mail e-mail: [hiroki@sanken.osaka-u.ac.jp](mailto:hiroki@sanken.osaka-u.ac.jp)

## I. INTRODUCTION

Progress in semiconductor devices has been largely due to advances in lithographic technologies. Exposure sources have been replaced with sources emitting shorter wavelengths to meet market demand. Since photolithography was first deployed for the mass production of semiconductor devices, the replacement of exposure sources has continued to shift toward shorter wavelengths. The current exposure tool in state-of-the-art production lines is the ArF excimer laser. However, optical lithography is reaching to its limits with the pattern sizes approaching less than 16 nm. To replace ArF immersion lithography, ionizing radiation, such as extreme ultraviolet (EUV) or an electron beam (EB), is the most promising exposure tool.

In the progress of lithographic technology, the concept of “chemical amplification” developed by Ito and Willson<sup>1</sup> has had a great impact on resist design and has been predicted to work well in next-generation lithography systems. Nowadays, the requirements for next-generation resist materials are so challenging that technical solutions have not yet been found. In particular, nanoscale resist topographies such as line width roughness (LWR) have become the most serious problem. The LWR target has been set to less than 1 nm for the 22 nm dynamic random access memory (DRAM) half pitch.<sup>2</sup> Also, the sensitivity of resists has been considered to be a very important factor, and its requirement is set to be 5-20 mJ/cm<sup>2</sup> for EUV and 50-60  $\mu\text{C}/\text{cm}^2$  for an EB.<sup>2</sup> Moreover, there is a trade-off relationship among resolution, sensitivity, and LWR. To meet these strict demands for next-generation lithography (NGL), the development of novel materials is required.

If a resolution of less than 22 nm is achieved using polymer-based resist materials, the line width will correspond to 5-6 monomer units of the polymer. In addition, the molecular sizes of a polymer are different, i.e., a polymer has a molecular weight distribution. On the other hand, molecular resists have smaller molecular sizes than polymer resists and no dispersion of the molecular weight. Therefore, a molecular resist materials are expected to exhibit better patterning properties in NGL systems.

Up to now, several different materials have been investigated as potential molecular resist materials<sup>3-5</sup>. Recently, Kudo and co-workers succeeded in the synthesis of a new ladder cyclic oligomer “noria” (water wheel in Latin)<sup>6</sup> and reported the synthesis and photochemical reactivity of noria derivatives containing *t*-butoxycarbonyl groups,<sup>7,8</sup> *t*-butylester groups,<sup>9</sup> acetal groups,<sup>10,11</sup> and adamantyl ester groups.<sup>12-15</sup> It was found that these noria derivatives had high photo-reactivity and produced clear line and space patterns with resolutions of 50-70 nm using an EB exposure tool and 26 nm using EUV exposure tool, respectively.<sup>8-15</sup>

To enhance the performance of molecular resist materials based on cyclic oligomers, we evaluated their lithographic performances such as sensitivity, resolution and LWR, using EUV and EB exposure systems. Furthermore, we also examined the etching durability of the synthesized molecular resist materials.

## **II. EXPERIMENTAL**

### **2.1. Materials**

Propylene glycol mono methyl ether acetate (PGMEA), propylene glycol methyl ether (PGME), and dyglyme without further purification were used as casting solvents. Triphenylsulfonium nonafluoromethanesulfonate (TPS-nf) without further purification was used as an acid generator.

### **2.2. Synthesis of cyclic oligomer derivatives with pendant adamantyl ester groups (noria-AD, noria-OEt-AD, noria-OMe-AD, calixarene dimer-AD, triple-ringed[14]arene-AD, pillar[5]arene-AD, $\beta$ -cyclodextrin-AD)**

Noria derivatives with pendant adamantyl ester moieties (noria-AD) were synthesized by the reaction of noria and 2-chloroacetyloxy-2-methyladamantane in accordance with a the previous report.<sup>14</sup> Other cyclic oligomer derivatives such as noria-OEt-AD, noria-OMe-AD, calixarene dimer-AD, triple-ringed[14]arene-AD, pillar[5]arene-AD, and  $\beta$ -cyclodextrin-AD were also synthesized by the same method.

### **2.3. Synthesis of noria derivatives with pendant cyclohexyl 2-propyl ether groups**

Noria derivatives with pendant cyclohexyl 2-propyl ether groups were synthesized by the reaction of noria and cyclohexyl vinyl ether according to a previous report.<sup>10</sup>

### **2.4. Resist film preparation**

Silicon wafers (Mitsubishi Materials Electronic Chemicals., n-type, <100>) were used as substrates for all samples. Eight kinds of cyclic oligomers and the acid generator were each dissolved in PGMEA, PGME, and dyglyme. The weight ratio of the constituents was cyclic oligomers/acid generator = 100/10. By adjusting the concentration of the resist solution as well as the spin speed, 100 nm resist films were prepared for sensitivity measurement, while resist films with a thickness of less than 100 nm were spun for resolution measurement.

### **2.5. Sensitivity of EUV exposure system**

To evaluate the resist performances, the Si wafers were primed with hexamethyldisilazane (HMDS). The resist solutions were filtered through a 0.20  $\mu\text{m}$  PTFE

syringe filter prior to spin-coating on silicon wafers. Spin-coating was performed at 3000 rpm for 30 s to form thin films on the silicon wafers. Then these spin-coated films were prebaked at 110 °C for 90 s. The film thickness was adjusted to 100 nm. The films were exposed to EUV (Energetic, EQ-10M).<sup>16</sup> The area of exposure was approximately 1 × 1 cm<sup>2</sup>. After the exposure, they were baked at 110 °C for 60 s. They were developed by dipping in tetramethylammonium hydroxide (TMAH) (2.38 wt%) solutions at 23 °C for 30 s and then rinsed in deionized water before drying. The resist film thickness was measured with an ET200 surface profiler to obtain sensitivity curves.

## 2.6. Patterning properties using EB exposure tool

For the SEM observation of resist performances, the Si wafers were primed with HMDS. The resist solutions were filtered through a 0.20 μm PTFE syringe filter prior to spin-coating on silicon wafers at 3000 rpm for 30 s to form thin films. The spin-coated films were then prebaked at 110 °C for 90 s under a N<sub>2</sub> gas flow. A water-soluble conducting polymer (Showa Denko, Espacer) was also spin-coated at 2000 rpm for 60 s before exposure. The films were exposed to a 75 kV EB (ELIONIX, ELS-7700). After the exposure, they were baked at a temperature of 110 °C for 60 s. They were developed by dipping in 2.38 N TMAH solutions at 23 °C for 30 s and then rinsed in deionized water for 30 s before drying. Resist patterns were recorded with a Hitachi-hitec S-5500 SEM. LWR measurements were performed using the standard LWR measurement algorithm on the Hitachi S5500 SEM. In the LWR measurement, the reported LWR values are average values taken from ten different lines with a 1 μm inspection length.

## 2.7. Etching durability measurement

The etching rates of the noria derivative resists were investigated using a reactive ion etching (RIE) plasma process. The plasma conditions were a 15 sccm CF<sub>4</sub> gas flow, a 5 sccm Ar gas flow, and an RF power of 100 W. The pressure in the process chamber was 1.0 Pa. Under these conditions, the etching rates for the noria and calixarene derivative resists were estimated.

# III. RESULTS AND DISCUSSION

## 3.1. Synthesis of resist materials 1-8.

We synthesized eight kinds of cyclic oligomers (Resists **1-8**) with pendant protecting groups. Figure 1 shows Resists 1-4, which were based on noria.<sup>6</sup> Resists **1** and **2** were prepared from noria derivatives with pendant adamantyl ester (AD) and cyclohexyl 2-propyl ether moieties, whose degrees of protecting groups (DP) were 40 and 23%, respectively. Resists **3** and **4** were prepared from noria-OEt<sup>17</sup> with AD (DP = 49%) and noria-OMe<sup>18</sup> with AD (DP = 44%), respectively. Figure 2 shows Resists 5-8, which were based on calixarene

dimer,<sup>19, 20</sup> triple-ringed[14]arene,<sup>21</sup>  $\beta$ -cyclodextrin,<sup>22</sup> and pillar[5]arene,<sup>23</sup> respectively. Resist **5** was based on calixarene dimer with AD (DP = 37%). Resist **6** was derived from triple-ringed[14]arene with pendant AD (DP = 30%). The  $\beta$ -cyclodextrin derivative with pendant AD (DP = 64) and the pillar[5]arene derivative with AD (DP = 35) also correspond to Resists **7** and **8**, respectively. These resist materials had good solubility and good film-forming properties.

### 3.2. Sensitivity of molecular resist materials Resists **1** ~ **8**

For the evaluation of resist performances, we examined the sensitivity of these resist materials using an EUV exposure tool. Solutions of Resists **1-4** containing 10 wt% TPS-nf as an acid generator and no amine in PGMEA were prepared and corresponding thin films with 100 nm thickness were obtained by spin-coating on the silicon wafers. The postexposure baking (PEB) temperature and time were 110 °C and 60 s, respectively. Their sensitivities were examined by measurement of the film thickness after the lithography process. These results are depicted in Figure 3.

These results show that the order of sensitivity was Resist **3** > Resist **1** > Resist **4** > Resist **2**, i.e., adamantyl ester group is superior to the cyclohexyl 2-propyl ether group. This is presumably because the enhancement of acid generation efficiency leads to the increase sensitivity of resist materials. As for the ionization channel, protons of acids are generated through deprotonation of base polymers.<sup>24</sup> Therefore, the acid generation efficiency highly depends on polymer structure. In previous study, the differences of acid generation efficiencies among poly(4-hydroxystyrene)(PHS), poly(4-bromostyrene), poly(4-chlorostyrene), poly(4-methylstyrene), poly( $\alpha$ -methylstyrene) and polystyrene were observed.<sup>25</sup> The acid generation efficiency depends on polymer structure in EB and EUV resists. This means that the modification of base polymers has a great effect on the acid generation efficiency. Also, the dependence of acid generation efficiency on protection ratio of hydroxyl groups in the ionization channel was investigated and it has clarified that the selection of protecting groups is important for the acid generation efficiency.<sup>26</sup> Especially, it has been reported that the acid yield of polyhydroxystyrene (PHS) protected by AD gradually increases with increasing protection ratio of hydroxyl groups<sup>27</sup> and that the radical cation of adamantane has comparable acidity to mineral acids.<sup>28</sup> Therefore, a radical cation of AD seems to produce a proton and a radical cation of adamantane. Thus, AD group could lead to the enhancement of acid generation efficiency, namely, resist sensitivity.

Next, the same examination was performed using Resists **5-8** with pendant AD moieties as protecting groups. Figure 4 shows the obtained sensitivity curves, which indicated that the order of sensitivity was Resist **7** > Resist **8**  $\doteq$  Resist **5** > Resist **6**. We expected that Resist **5** would exhibit higher sensitivity than the other resist materials because the diameter of

the calixarene dimer is smaller than that of the other cyclic oligomers. However, Resist **5** shows the lowest sensitivity after Resist **6**. This result means that cyclic oligomers containing large holes might exhibit high sensitivity in NGL lithography systems employing EUV and EB exposure. Therefore, we also expected that the pillar[5]arene derivative with pendant AD (Resist **8**) would show high sensitivity. However, the sensitivity of Resist **8** was inferior to that of Resist **3**.

Consideration of the skeletons of pillar[5]arene and noria suggests that the size of the hole in cyclic oligomers is a key indicator of sensitivity. The cyclic oligomer pillar[5]arene doesn't have a large hole with a fixed size because molecular motion of aromatic moieties occur. However, noria, noria-OMe, and noria-OEt do have a large hole with a fixed size. These results mean that cyclic oligomers a large hole with a fixed size may be suitable for obtaining higher resolution using NGL.

### **3.3. Patterning properties of Resists 1-8 using EB exposure tool.**

Patterning experiments were also carried out using an EB. Figure 5 shows SEM micrographs of line and space patterns delineated on Resists **1**, **4** and **5**. As predicted from the sensitivity results, the sensitivity of Resist **1** was higher than that of Resist **4**. Relatively fine patterns in both Resists **1** and **4** were obtained upon exposure to an EB. In Resist **1**, the best line width and pitch were 40 and 200 nm, respectively. On the other hand, the best line width and pitch were 50 and 120 nm in Resist **4**, respectively. These patterns required a dose of 100  $\mu\text{C}/\text{cm}^2$ . Dense fine patterns of size less than 32 nm could not be obtained. Pattern collapse were observed as shown in Figure 5 because the film thickness is around 100 nm. If the processing conditions are optimized, dense patterns with a size of less than 22 nm are expected to be obtained in Resist **4**.

Figure 6 shows SEM micrographs of line and space patterns delineated on Resists **5**, **6**, and **8**. As predicted by the sensitivity results, the sensitivity of Resist **5** was higher than those of Resists **6** and **8**. When Resist **8** containing 10 wt% TPS-nf was used, a semi-isolated pattern with a line width of 20 nm (pitch: 100 nm) was delineated at a dose of 200  $\mu\text{C}/\text{cm}^2$ . This pattern had the best resolution under these conditions. In addition, the patterning result of Resist **5** shows a semi-isolated pattern with a line width of 40 nm (pitch: 100 nm), which was obtained at a dose of 100  $\mu\text{C}/\text{cm}^2$ . In Resist **6**, line and space pattern had a half pitch of 60 nm. This pattern required a dose of 500  $\mu\text{C}/\text{cm}^2$ . These results indicate that these resists of noria and calixarene dimer derivatives have high potential for providing exceptional resolution as future positive tone EUV and EB resist materials.

Although these molecular resists have the potential to produce higher resolution patterns, their values of line-edge roughness remain too high at present. The  $3\sigma$  LWRs of the

noria and calixarene derivative resists were calculated from the SEM images. As shown in Figure 5, LWRs of Resists **1** and **4** were 7.5 nm (line width 80 nm, pitch 200 nm) and 6.3 nm (line width 50 nm, pitch 120 nm), respectively. The LWRs of Resists **5**, **6**, and **8** were 5.3 nm (line width 50 nm, pitch 100 nm), 8.0 nm (line width 80 nm, pitch 200 nm) and 6.1 nm (line width 40 nm, pitch 100 nm), respectively, as shown in Figure 6. These results showed that the LWRs of the novel calixarene dimer resists are similar to that of a polymer resist. Although the LWRs of the noria and calixarene dimer derivative resists were not superior to that of a polymer resist, their lithographic performance such as LWR has the potential to be improved by modification of the molecular structure. We intend to examine in detail whether a higher resolution and lower LWR can be obtained by using noria derivatives containing other protecting groups. Further modification of the material design and optimization of the processing conditions are in progress.

#### **3.4. Etching durability of synthesized resist materials**

Etching durability becomes increasingly important with increasing resolution because thinner films are required to avoid pattern collapse. The etching durability of molecular resists is generally less than those of polymer resists. Because the noria derivative structures include more rigid cyclic molecules, such as cavitands and carcerands, than calixarene dimer derivatives, they are expected to have higher etching durability as molecular glass resists. Also, the patterns might be broken down during etching in positive-tone molecular glass resists owing to their insufficient structural stability. Therefore, the etching rates of the noria and calixarene dimer derivative resists were investigated using the RIE plasma process. Figure 7 (a) and 7 (b) show the etching rates of the noria derivative resists (Resists **1-4**), calixarene dimer derivatives and  $\beta$ -cyclodextrin (Resists **5-8**), respectively. The plasma conditions were a 15 sccm  $\text{CF}_4$  gas flow, a 5 sccm Ar gas flow, and an RF power of 100 W. The pressure in the process chamber was 1.0 Pa. The etching rates of the noria and calixarene dimer derivative resists are summarized in Table 1. The etching durability of the noria and calixarene dimer derivative resists was higher than that of resist materials such as PMMA. Also, the etching rates of the noria and calixarene dimer derivative resists were similar to those of conventional resist materials such as ZEP520A and UVIII. Furthermore, small modifications of the noria and calixarene dimer derivative resists hardly affected the etch durability. Therefore, noria and calixarene dimer derivative resists can enhance lithographic performance without sacrificing etch durability. Noria and calixarene dimer derivative resists have the potential to offer exceptional resolution as future positive-tone EUV and EB resist materials.

#### **IV. CONCLUSION**

We developed positive-tone chemically amplified molecular resist materials based on cyclic oligomers such as noria, calixarene dimer, cyclodextrin, and pillar[5]arene. The lithographic performances such as sensitivity, etch durability, and patterning properties were evaluated under EUV and EB exposure. We clarified that a small modification of noria resists can cause a significant change in sensitivity. In particular, noria derivative, which modified by the combination AD groups and ethoxy groups, can be used to improve resist sensitivity. Furthermore, the etching rates of noria derivatives are similar to those of conventional resist materials such as ZEP520A and UVIII. From the comparison among synthesized cyclic oligomers, we concluded that these oligomers have the potential to offer exceptional resolution as future positive tone EUV and EB resist materials.

### **Acknowledgement**

The authors wish to thank Prof. Tadatomi Nishikubo for his guidance, helpful suggestions, and warm encouragement throughout their research. This work was partly performed under the Cooperative Research Program "Network Joint Research Center for Materials and Devices"



## References

- 1 H. Ito and C. G. Willson, *Polym. Eng. Sci.* **23** (1983) 1012.
- 2 International Technology Roadmap for Semiconductors, <http://www.itrs.net>, (accessed online 2013).
- 3 F. Diederich, and C. Thilgen, *Science* **271** (1996) 317.
- 4 M. Yoshiiwa, H. Kageyama, Y. Shiota, F. Wakaya, K. Gamo, and M. Takai, *Appl. Phys. Lett.* **69** (1996) 2605.
- 5 J. Fujita, Y. Ohnishi, Y. Ochiai, and S. Matsui, *Appl. Phys. Lett.* **68** (1996) 1297.
- 6 H. Kudo, R. Hayashi, K. Mitani, T. Yokozawa, N. C. Kasuga, and T. Nishikubo, *Angew. Chem. Int. Ed.* **45** (2006) 7948.
- 7 X. André, J. K. Lee, A. D. Silva, C. K. Ober, H. B. Cao, H. Deng, H. Kudo, and T. Nishikubo, *Proc. SPIE* **6519** (2007) 65194B.
- 8 H. Kudo and T. Nishikubo, *Polym. J.* **41** (2009) 569.
- 9 H. Kudo, D. Watanabe, T. Nishikubo, K. Maruyama, D. Shimizu, T. Kai, T. Shimokawa, and C. K. Ober: *J. Mater. Chem.* **18** (2008) 3588.
- 10 H. Kudo, M. Jinguji, T. Nishikubo, H. Oizumi, and T. Itani, *J. Photopolym. Sci. Technol.* **23** (2010) 657.
- 11 H. Kudo, K. Mitani, S. Koyama, and T. Nishikubo, *Bull. Chem. Soc. Jpn.* **77** (2004) 819.
- 12 T. Nishikubo, H. Kudo, Y. Suyama, H. Oizumi, and T. Itani, *J. Photopolym. Sci. Technol.* **22** (2009) 73.
- 13 H. Seki, H. Kudo, H. Oizumi, T. Itani, and T. Nishikubo, *Jpn. J. Appl. Phys.* **50** (2011) 121602.
- 14 N. Niina, H. Kudo, H. Oizumi, T. Itani, and T. Nishikubo, *Thin Solid Films* **534** (2013) 459.
- 15 H. Kudo, Y. Suyama, T. Nishikubo, H. Oizumi, and T. Itani, *J. Mater. Chem.* **20** (2010) 4445.
- 16 S. F. Horne, M. M. Besen, D. K. Smith, P. A. Blackborow, and R. D'Agostino, *Proc. SPIE* **6151** (2006) 61510P.
- 17 N. Nobumitsu, H. Kudo, and T. Nishikubo, *Chem. Lett.* **38** (2009) 1198.
- 18 N. Niina, H. Kudo, K. Maruyama, T. Kai, T. Shimokawa, H. Oizumi, T. Itani, and T. Nishikubo, *Polym. J.* **43** (2011) 407.
- 19 T. Nishikubo, and H. Kudo, *Japan Patent* (2008) JP2008-280269A.
- 20 H. Yamada, T. Ikeda, T. Mizuta, and T. Haino, *Org. Lett.* **17** (2012) 4510.
- 21 H. Seki, S. Kuwabara, H. Kudo, and T. Nishikubo, *Chem. Lett.* **41** (2012) 699.
- 22 F. Davis, and S. Higson, *Macrocycles: Construction, Chemistry and Nanotechnology Application*, John Wiley & Sons. Ltd (2011).
- 23 T. Ogoshi, S. Kanai, S. Fujinami, T. Yamagishi and Y. Nakamoto, *J. Am. Chem. Soc.* **130**

- (2008) 5022.
- 24 T. Kozawa, S. Nagahara, Y. Yoshida and S. Tagawa, *J. Vac. Sci. Technol.* **B15**, 2582 (1997).
- 25 H. Yamamoto, A. Nakano, K. Okamoto, T. Kozawa and S. Tagawa, *Jpn. J. Appl. Phys.* **43**, (2004) 3971.
- 26 H. Yamamoto, T. Kozawa, A. Nakano, K. Okamoto, S. Tagawa, T. Ando, M. Sato, and H. Komano, *Jpn. J. Appl. Phys.* **44** (2005) 5836.
- 27 H. Yamamoto, T. Kozawa, A. Nakano, K. Okamoto, S. Tagawa, T. Ando, M. Sato, and H. Komano, *J. Vac. Sci. Technol. B* **23** (2005) 2728.
- 28 M. Mella, M. Freccero, T. Soldi, E. Fasani, and A. Albini, *J. Org. Chem.* **61** (1996) 1413.

Figure 1. Resist materials based on noria.

Figure 2. Sensitivity curves of noria derivative resists (Resist **1-4**) upon exposure to EB. The noria derivative resists contain 10 wt% acid generator and no amine. The postexposure baking (PEB) temperature and time were 90 °C and 60 s, respectively.

Figure 3. SEM micrographs of line and space patterns delineated on Resists **1- 4**.

Figure 4. Estimated etching rates of noria derivative resists (Resists **1-4**). The plasma conditions were a 15 sccm CF<sub>4</sub> gas flow, a 5 sccm Ar gas flow, and an RF power of 100 W. The pressure in the process chamber was 1.0 Pa.

Table 1. Relative etching rates of noria derivative(Resists **1-4**), normalized to PHS.

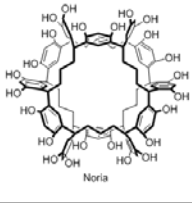
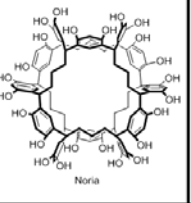
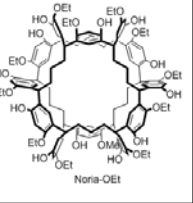
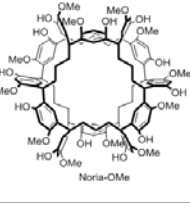
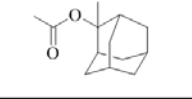
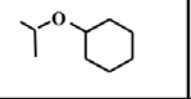
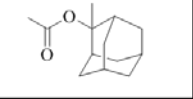
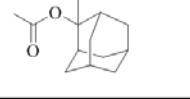
Sample Name	Resist 1	Resist 2	Resist 3	Resist 4
Core Structure	 Noria	 Noria	 Noria-OEt	 Noria-OMe
Protecting group				
Protecting ratio (%)	40	23	49	44
Casting Solvent	PGMEA	PGME	PGMEA	PGMEA

Fig. 1

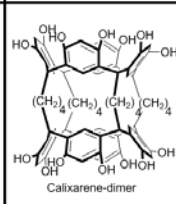
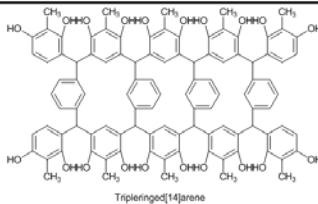
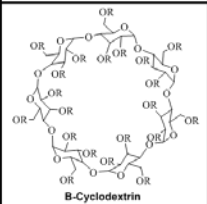
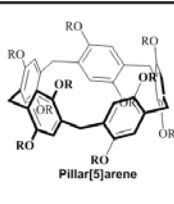
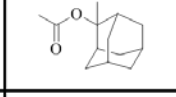
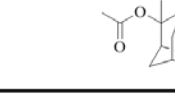
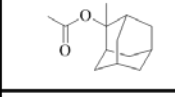
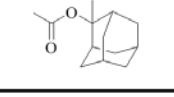
Sample Name	Resist 5	Resist 6	Resist 7	Resist 8
Core Structure	 Calixarene-dimer	 Tripleringed[14]arene	 B-Cyclodextrin	 Pillar[5]arene
Protecting group				
Protecting ratio (%)	37	30	64	35
Casting Solvent	PGMEA	PGMEA	Dyglyme	PGMEA

Fig. 2

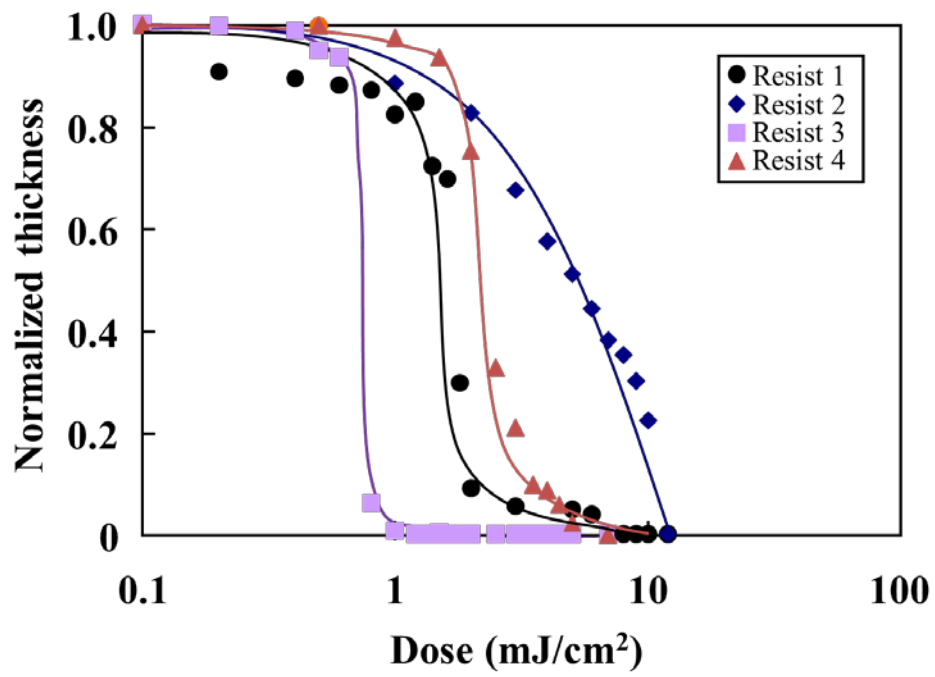


Fig. 3

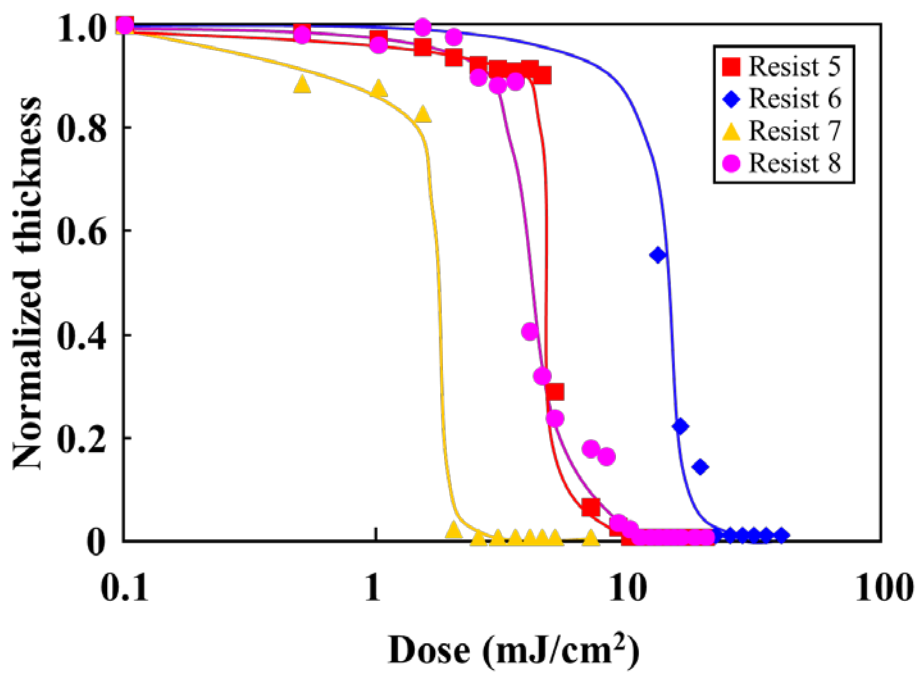


Fig. 4

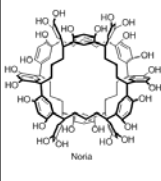
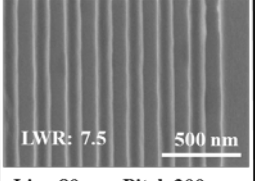
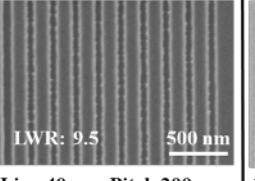
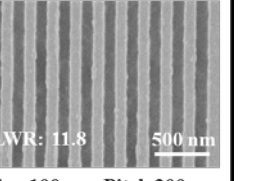
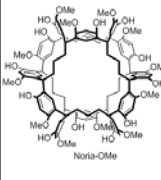
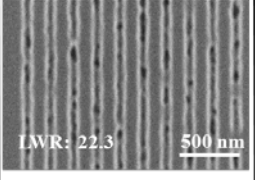
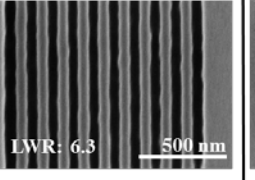
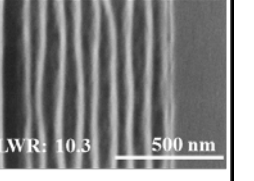

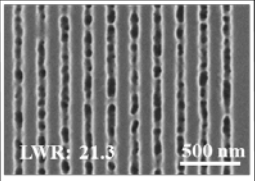
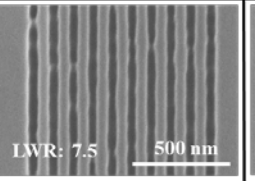
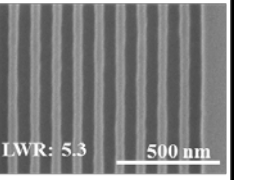
	Exposure dose 40 $\mu\text{C}/\text{cm}^2$	Exposure dose 100 $\mu\text{C}/\text{cm}^2$	Exposure dose 200 $\mu\text{C}/\text{cm}^2$
 <p>Noria</p>	 LWR: 7.5 <u>500 nm</u> <b>Line 80 nm, Pitch 200 nm</b>	 LWR: 9.5 <u>500 nm</u> <b>Line 40 nm, Pitch 200 nm</b>	 LWR: 11.8 <u>500 nm</u> <b>Line 100 nm, Pitch 200 nm</b>
 <p>Noria-OMe</p>	 LWR: 22.3 <u>500 nm</u> <b>Line 50 nm, Pitch 200 nm</b>	 LWR: 6.3 <u>500 nm</u> <b>Line 50 nm, Pitch 120 nm</b>	 LWR: 10.3 <u>500 nm</u> <b>Line 30 nm, Pitch 80 nm</b>
 <p>Calixarene-dimer</p>	 LWR: 21.3 <u>500 nm</u> <b>Line 50 nm, Pitch 200 nm</b>	 LWR: 7.5 <u>500 nm</u> <b>Line 40 nm, Pitch 100 nm</b>	 LWR: 5.3 <u>500 nm</u> <b>Line 50 nm, Pitch 100 nm</b>

Fig. 5

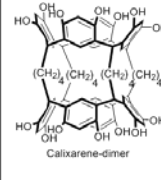
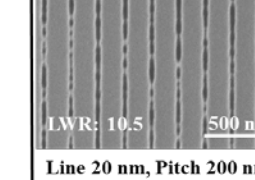
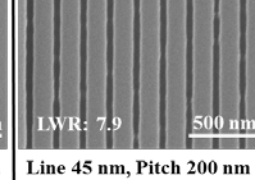
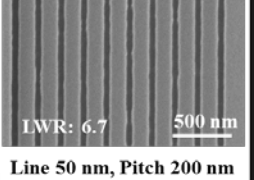
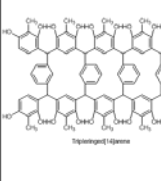
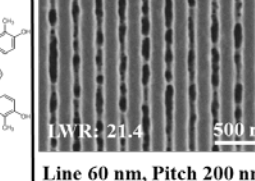
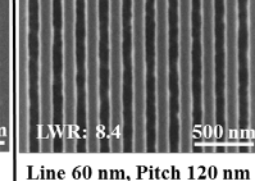
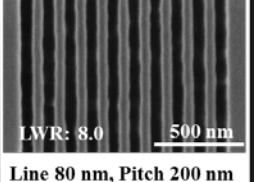
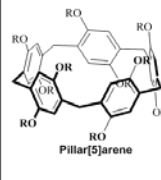
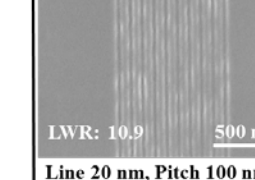
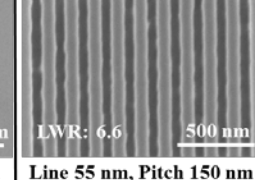
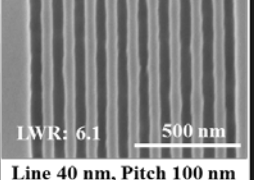
	Exposure dose 200 $\mu\text{C}/\text{cm}^2$	Exposure dose 300 $\mu\text{C}/\text{cm}^2$	Exposure dose 500 $\mu\text{C}/\text{cm}^2$
 <p>Calixarene-dimer</p>	 LWR: 10.5 <u>500 nm</u> <b>Line 20 nm, Pitch 200 nm</b>	 LWR: 7.9 <u>500 nm</u> <b>Line 45 nm, Pitch 200 nm</b>	 LWR: 6.7 <u>500 nm</u> <b>Line 50 nm, Pitch 200 nm</b>
 <p>Tetra[arylethylene]diphenylene</p>	 LWR: 21.4 <u>500 nm</u> <b>Line 60 nm, Pitch 200 nm</b>	 LWR: 8.4 <u>500 nm</u> <b>Line 60 nm, Pitch 120 nm</b>	 LWR: 8.0 <u>500 nm</u> <b>Line 80 nm, Pitch 200 nm</b>
 <p>Pillar[5]arene</p>	 LWR: 10.9 <u>500 nm</u> <b>Line 20 nm, Pitch 100 nm</b>	 LWR: 6.6 <u>500 nm</u> <b>Line 55 nm, Pitch 150 nm</b>	 LWR: 6.1 <u>500 nm</u> <b>Line 40 nm, Pitch 100 nm</b>

Fig. 6

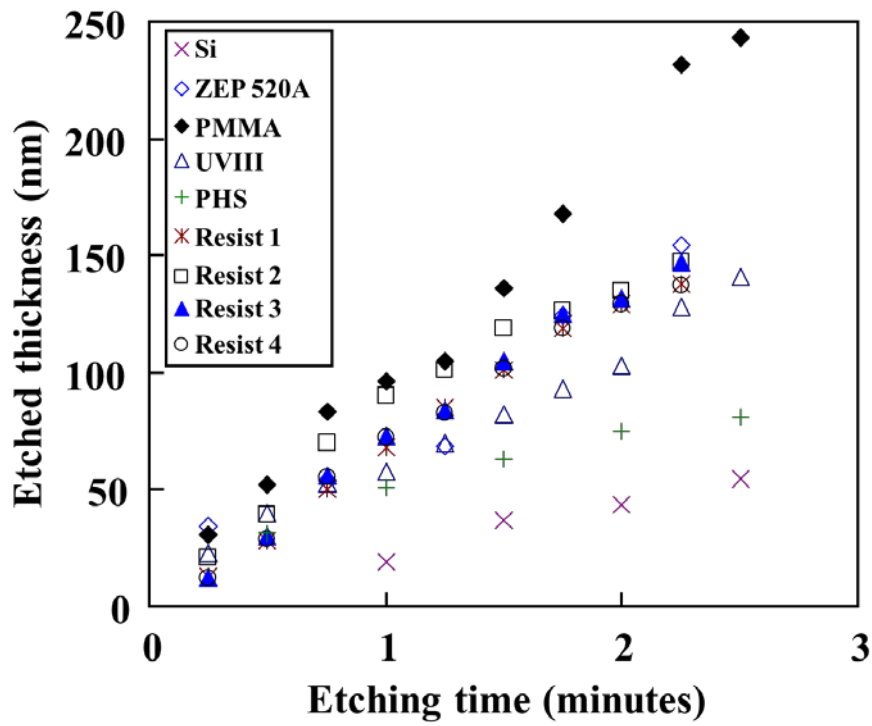


Fig. 7(a)

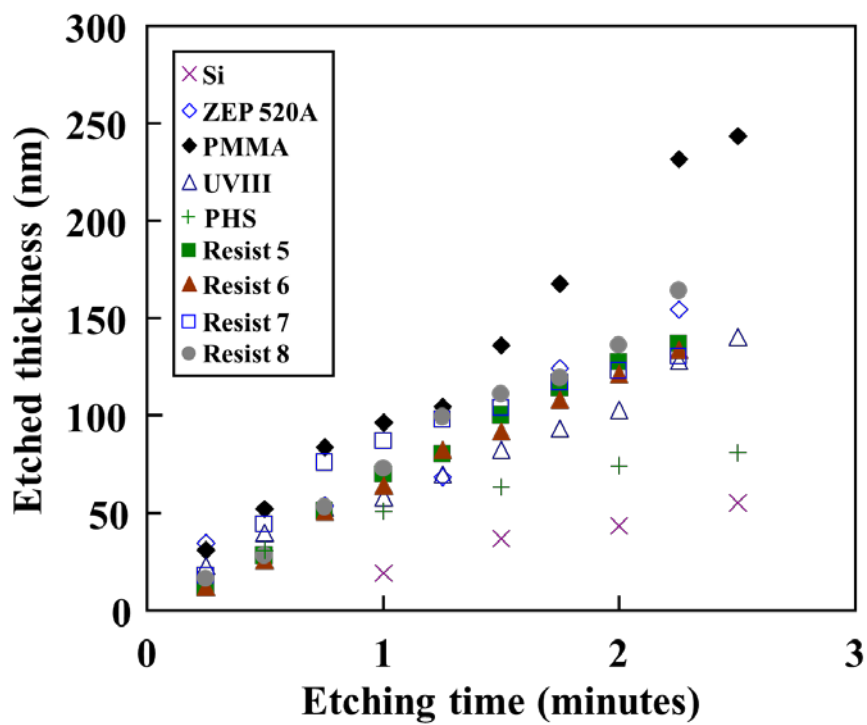


Fig. 7(b)

Table 1

<b>Sample</b>	<b>Rate (nm/s)</b>
<b>PMMA</b>	<b>97</b>
<b>ZEP 520A</b>	<b>54</b>
<b>UVIII</b>	<b>56</b>
<b>Si</b>	<b>23</b>
<b>PHS</b>	<b>36</b>
<b>Resist 1</b>	<b>65</b>
<b>Resist 2</b>	<b>73</b>
<b>Resist 3</b>	<b>68</b>
<b>Resist 4</b>	<b>65</b>
<b>Resist 5</b>	<b>64</b>
<b>Resist 6</b>	<b>67</b>
<b>Resist 7</b>	<b>61</b>
<b>Resist 8</b>	<b>71</b>